PROCEEDINGS OF SCIENCE

Impact of top mass on top differential distributions

Toni Mäkelä,[a,*] **André Hoang,**[b] **Katerina Lipka**[c,d] **and Sven-Olaf Moch**[e]

[a] *National Centre for Nuclear Research, Pasteura 7, 02-093 Warsaw, Poland*
[b] *Fakultät für Physik, Universität Wien, Boltzmanngasse 5, A-1090 Wien, Austria*
[c] *Deutsches Elektronen-Synchrotron, Notkestraße 85, D-22607 Hamburg, Germany*
[d] *Fakultät für Mathematik und Naturwissenschaften, Bergische Universität Wuppertal, Gaussstrassse 20, 42119 Wuppertal, Germany*
[e] *II. Institut für Theoretische Physik, Universität Hamburg, Luruper Chaussee 149, 22761 Hamburg, Germany*

E-mail: Toni.Makela@ncbj.gov.pl

The next-to-leading order single-differential top quark-antiquark pair production cross section predictions are examined consistently using short-distance top quark mass schemes, with the evolution of the mass of the top quark performed in the MSR scheme $m_t^{\mathrm{MSR}}(\mu)$ for scales μ below the $\overline{\mathrm{MS}}$ top quark mass $\overline{m}_t(\overline{m}_t)$, and in the $\overline{\mathrm{MS}}$ scheme $\overline{m}_t(\mu)$ for scales above. The implementation of a mass renormalization scale independent of the strong coupling renormalization scale and factorization scale in quantum chromodynamics allows investigating independent dynamical scale variations, and a scale choice of $R \sim 80$ GeV is demonstrated to be important for the stability of the cross-section predictions in the low top quark-antiquark pair invariant mass range. Moreover, a choice of semi-dynamical renormalization and factorization scales is preferred, and the findings are demonstrated in a theoretically consistent extraction of the top quark MSR mass from experimental data.

The eleventh Large Hadron Collider Physics Conference - LHCP 2023
22-26 May, 2023
Belgrade, Serbia

*Speaker

PoS(LHCP2023)022

The top quark mass m_{t} is one of the fundamental parameters of the Standard Model, and has a significant impact on various predictions both directly and via higher-order corrections. Yet, quark masses are formal parameters of the Lagrangian of quantum chromodynamics (QCD), and dependent on a choice of renormalization scheme. While the frequently used pole mass $m_{\mathrm{t}}^{\mathrm{pole}}$, based on the picture of an on-shell observable particle, allows for consistent cross section field theory computations, it suffers from an infrared sensitivity of the order of the scale of QCD known as the renormalon ambiguity [1–3]. On the other hand, this issue does not concern the so-called short-distance masses such as the $\overline{\mathrm{MS}}$ mass $\overline{m}_{\mathrm{t}}(\mu_m)$ and the MSR mass $m_{\mathrm{t}}^{\mathrm{MSR}}(R)$ [4, 5], where the mass renormalization scales μ_m and R, respectively, act as finite resolution scales. In their case, real and virtual self-energy radiation are treated inclusively at scales below the mass renormalization scale. The freedom to adopt suitable choices for μ_m and R can potentially enhance the precision of top mass sensitive observables, in particular for predictions at lower orders where it leads to a systematic absorption of sizeable corrections into the quark mass parameter. However, the dependence on the mass renormalization scales necessitates proper scale setting for the extraction of theoretically well-defined masses from cross section measurements to avoid the appearance of large logarithms. The present work is the first concurrent investigation of the invariant mass of the $\mathrm{t\bar{t}}$ pair $m_{\mathrm{t\bar{t}}}$, on the MSR mass scale R and the $\overline{\mathrm{MS}}$ mass scale μ_m, accounting for QCD corrections. Further details and results of the investigations are provided in Ref. [6].

The relation of the pole and $\overline{\mathrm{MS}}$ masses reads $m_{\mathrm{t}}^{\mathrm{pole}} = \overline{m}_{\mathrm{t}}(\mu_m)\left(1 + \sum_{n=1} d_n^{\overline{\mathrm{MS}}}(\mu_m)(a_S(\mu_m))^n\right)$, where $d_n^{\overline{\mathrm{MS}}}(\mu_m)$ are perturbative coefficients and $a_S \equiv \alpha_S/\pi$. The pole and MSR masses are related via $m_{\mathrm{t}}^{\mathrm{pole}} = m_{\mathrm{t}}^{\mathrm{MSR}}(R) + R\sum_{n=1}^{\infty} d_n^{\mathrm{MSR}}(a_S(R))^n$. Then $\lim_{R\to 0} m_{\mathrm{t}}^{\mathrm{MSR}}(R) \to m_{\mathrm{t}}^{\mathrm{pole}}$, and $\lim_{R\to\overline{m}_{\mathrm{t}}(\overline{m}_{\mathrm{t}})} m_{\mathrm{t}}^{\mathrm{MSR}}(R) \to \overline{m}_{\mathrm{t}}(\overline{m}_{\mathrm{t}})$ up to a small matching correction, with the latter obtained by integrating out top quark loop corrections at $R \lesssim \overline{m}_{\mathrm{t}}(\overline{m}_{\mathrm{t}})$ [7]. While the μ_m evolution of $\overline{m}_{\mathrm{t}}(\mu_m)$ is logarithmic, the R-evolution of $m_{\mathrm{t}}^{\mathrm{MSR}}(R)$ is linear, and designed to capture the correct physical logarithms for observables with m_{t} dependence generated at dynamical scales $R < m_{\mathrm{t}}$, such as resonances, thresholds and low-energy endpoints [8]. At dynamical scales of order and larger than m_{t}, the $\overline{\mathrm{MS}}$ mass and evolution are used. Based on Refs. [9, 10], the top quark-antiquark ($\mathrm{t\bar{t}}$) production cross section as a function of the $\mathrm{t\bar{t}}$ system invariant mass $m_{\mathrm{t\bar{t}}}$ at next-to-leading order (NLO) is given by

$$\frac{d\sigma}{dm_{\mathrm{t\bar{t}}}} = a_S^2\frac{d\sigma^{(0)}}{dm_{\mathrm{t\bar{t}}}}(m,\mu_r,\mu_f) + a_S^3\frac{d\sigma^{(1)}}{dm_{\mathrm{t\bar{t}}}}(m,\mu_r,\mu_f) + a_S^3\tilde{R}d_1\frac{d}{dm_{\mathrm{t}}}\left(\frac{d\sigma^{(0)}(m_{\mathrm{t}},\mu_r,\mu_f)}{dm_{\mathrm{t\bar{t}}}}\right)\Bigg|_{m_{\mathrm{t}}=m}, \quad (1)$$

with $\sigma^{(0)}$ the leading order (LO) and $\sigma^{(1)}$ the NLO cross section in the pole mass scheme, and the short-distance schemes are implemented at NLO via the derivative term. Note that the renormalization (factorization) scale μ_r (μ_f) is independent of R or μ_m and $a_S = a_S(\mu_r)$. Furthermore,

$$(m, d_1, \tilde{R}) = \begin{cases}(m_{\mathrm{t}}^{\mathrm{MSR}}(R),\ d_1^{\mathrm{MSR}},\ R), & \text{in the MSR regime } (R < \overline{m}_{\mathrm{t}}(\overline{m}_{\mathrm{t}})),\\ (\overline{m}_{\mathrm{t}}(\mu_m),\ d_1^{\overline{\mathrm{MS}}}(\mu_m),\ \overline{m}_{\mathrm{t}}(\mu_m)), & \text{in the } \overline{\mathrm{MS}} \text{ regime } (R > \overline{m}_{\mathrm{t}}(\overline{m}_{\mathrm{t}})).\end{cases} \quad (2)$$

In the context of the present work, Eq. (1) is implemented into MCFM v6.8 [11, 12].

The implementation of the mass renormalization scales independently from μ_r and μ_f allows the first investigation of the dependence of the $m_{\mathrm{t\bar{t}}}$ distribution on the scale R. Fig. 1 shows the

$d\sigma/dm_{t\bar{t}}$ cross section in the range $m_{t\bar{t}} \in [300, 333]$ GeV at leading-order (LO) and NLO, as well as the ratio of the NLO to the LO cross section in the range $m_{t\bar{t}} \in [333, 366]$ GeV. Note that these ranges contain high sensitivity to m_t. The cross section for the range $m_{t\bar{t}} \in [300, 333]$ GeV, i.e. the region below the $t\bar{t}$ production threshold, is zero for $R < 60$ GeV, corresponding to $2m_t^{MSR}(R) > 333$ GeV. Non-zero contributions appear in the $m_{t\bar{t}} \in [300, 333]$ GeV range only at large R or when using the $\overline{MS}$ mass, corresponding to smaller values of $m_t^{MSR}(R)$ or $\overline{m}_t(\mu_m)$. The LO contribution is zero or positive throughout the probed range of R and μ_m, but the quick decrease of the derivative terms in Eq. (1) in contrast to the slow increase of the positive contributions leads to unphysical negative values of the NLO cross section in this kinematic range. This was also pointed out in the investigations of the $\overline{MS}$ scheme performed in Ref. [13]. Since $t\bar{t}$ production in the range $m_{t\bar{t}} \in [300, 333]$ GeV is impossible, the results in Fig. 1 also indicate that values of R above 80 GeV should be avoided. Therefore, the $\overline{MS}$ mass should not be used if the $t\bar{t}$ cross section in this $m_{t\bar{t}}$ range is included in the experimental analysis. The conclusion holds even in the presence of quasi-bound state effects, since these provide a more precise prediction of the $t\bar{t}$ production threshold located at $m_{t\bar{t}}$ values above 333 GeV. A further feature of the $m_{t\bar{t}} \in [300, 333]$ GeV range is the rapid increase of the cross section at $\mu_m \gtrsim 410$ GeV. This occurs when $\overline{m}_t(\mu_m)$ becomes so small, that LO $t\bar{t}$ production is possible even below 300 GeV. Furthermore, the ratio of the predictions at NLO to those at LO decreases substantially with increasing R, implying that the impact of the NLO corrections is small at these R. Particularly, with $R \in [60, 80]$ GeV, the cross section changes only little as a function of R. On the other hand, the impact of the higher-order QCD corrections, including the quasi-bound state corrections, would be sizeable at very small R. They are essentially maximized in the pole scheme which is closely mimicked by the result at $R = 1$ GeV. Additionally, the differences between the curves corresponding to smaller or larger central μ_r and μ_f values remain small. This motivates setting the central values of R, μ_r and μ_f to around 80 GeV near the peak of the $m_{t\bar{t}}$ distribution to obtain predictions that are robust against scale variations in the following extraction of the top quark MSR mass.

An extraction of $m_t^{MSR}(R)$ is performed from the single-differential $t\bar{t}$ production cross section measured by the CMS Collaboration in pp collisions at $\sqrt{s} = 13$ TeV [14], corresponding to an integrated luminosity of 35.9 fb^{-1}. The cross section is provided in the ranges $m_{t\bar{t}} < 420$ GeV, $m_{t\bar{t}} \in [420, 550]$ GeV, $m_{t\bar{t}} \in [550, 810]$ GeV and $m_{t\bar{t}} > 810$ GeV. The top quark MSR mass is extracted by fitting the predicted $t\bar{t}$ production cross section, computed with the ABMP16 5 flavor PDF [15] at NLO and assuming $R = 80$ GeV, to the experimental data. Since m_t values extracted at different scales are unambiguously related by renormalization group equations and matching relations, the resulting $m_t^{MSR}(80\,\text{GeV})$ is evolved to the reference scale of $R = 1$ GeV, as well as translated to $\overline{m}_t(\overline{m}_t)$. The fit uncertainty is obtained via the $\Delta\chi^2 = 1$ tolerance criterion. The uncertainty in the initial choice of R is estimated by repeating the fits assuming $R = 60$ GeV and 100 GeV, and taking the difference of the masses evolved to the reference scales to the respective results of the $R = 80$ GeV fit. The μ_r, μ_f uncertainty is obtained by independently varying the scales by factors of $2^{\pm 1}$, avoiding cases where one scale is multiplied by 2 and the other by 1/2, and constructing an envelope.

With $\mu_r = \mu_f = m_t^{MSR}(80\,\text{GeV})$ throughout the $m_{t\bar{t}}$ distribution, evolving the obtained $m_t^{MSR}(80\,\text{GeV})$ to $R = 1$ GeV yields $m_t^{MSR}(1\,\text{GeV}) = 173.2 \pm 0.6\,(\text{fit})^{+0.4}_{-0.6}\,(\mu_r, \mu_f)^{+0.4}_{-0.5}\,(R)$ GeV. This translates into $\overline{m}_t(\overline{m}_t) = 163.3^{+0.8}_{-1.0}$ GeV, which is compatible with the $\overline{m}_t(\overline{m}_t) = 162.1^{+1.0}_{-1.0}$ GeV

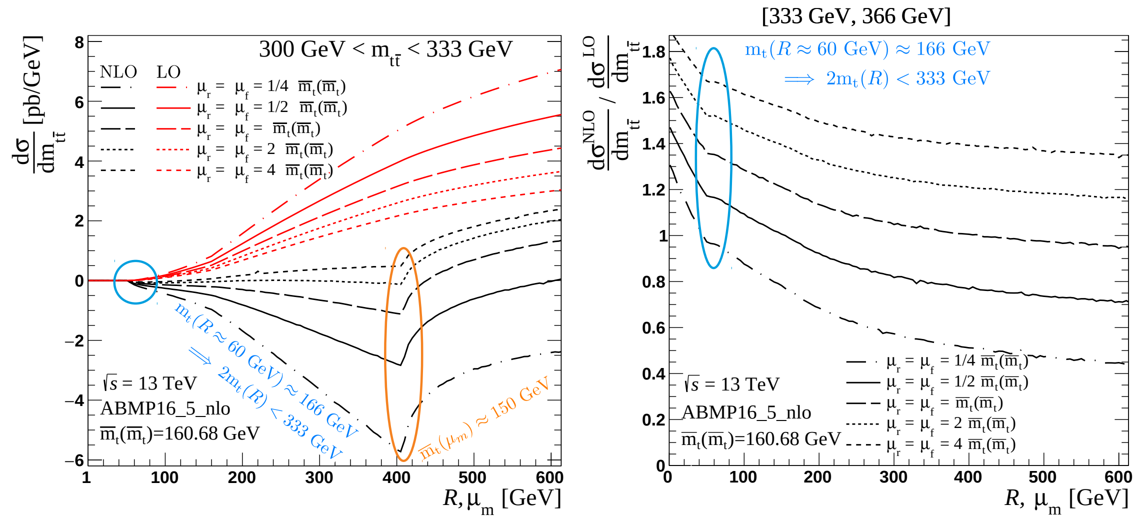

Figure 1: *Left:* The $m_{t\bar{t}} \in [300, 333]$ GeV range of the $m_{t\bar{t}}$ distribution. There is no $t\bar{t}$ production at $R \lesssim 60$ GeV, but the region above it suffers from the lack of Coulomb corrections. The discontinuity at $\mu_m \gtrsim 410$ GeV is due to the $t\bar{t}$ production threshold becoming artificially low, and such high values of the scale μ_m should be avoided. *Right:* The ratio of the NLO and LO cross sections in the $m_{t\bar{t}} \in [333, 366]$ GeV range. The transition from a region suffering from the missing Coulomb corrections to a more stable region where the threshold effects become less important is seen at $R \gtrsim 60$ GeV (blue). Additionally, small values of μ_r, μ_f are observed to stabilize the prediction quickly as a function of R or μ_m.

obtained at NLO in the ABMP16 5-flavor PDF set [15]. However, it disagrees with Ref. [16], where $m_t^{\text{pole}} = 170.5 \pm 0.8$ GeV was obtained, translating into $m_t^{\text{MSR}}(1\,\text{GeV}) = 170.2 \pm 0.8$ GeV and interpreting the pole mass [16] as the asymptotic pole mass [8]. To investigate the difference, an alternative fit is performed with R set directly to 1 GeV, instead of setting the initial value to $R = 80$ GeV and evolving the extracted $m_t^{\text{MSR}}(80\,\text{GeV})$ to $R = 1$ GeV. This results in $m_t^{\text{MSR}}(1\,\text{GeV}) = 170.1 \pm 0.6\,(\text{fit})^{+1.1}_{-0.9}\,(\mu_r, \mu_f)$ GeV, which is compatible with Ref. [16]. Since $m_t^{\text{MSR}}(1\,\text{GeV})$ approximates the pole scheme, this observation confirms the conclusion that the use of the pole scheme, or the MSR scheme with very small initial values of R, leads to less reliable results in a fixed-order QCD at NLO, where the resummation of quasi-bound state effects is missing.

Finally, to investigate the effect of using small μ_r and μ_f near the peak of the $m_{t\bar{t}}$ distribution, a fit is performed with the central choices of $\mu_r = \mu_f = m_t^{\text{MSR}}(80\,\text{GeV})/2$ for $m_{t\bar{t}} < 420$ GeV and $\mu_r = \mu_f = m_t^{\text{MSR}}(80\,\text{GeV})$ for $m_{t\bar{t}} > 420$ GeV. This results in $m_t^{\text{MSR}}(1\,\text{GeV}) = 174.8 \pm 0.5\,(\text{fit})^{+0.2}_{-0.4}\,(\mu_r, \mu_f)^{+0.2}_{-0.3}\,(R)$ GeV. As expected from the present investigations, the setting increases robustness against scale variations. While a comprehensive understanding of m_t extracted from cross section measurements will require the quasi-boundstate corrections and the resummation of soft gluon effects to be thoroughly investigated and accounted for, following e.g. Ref. [17], the present results indicate that proper scheme and scale choices are of key importance, affecting both the size of the higher-order corrections as well as the resulting value of the extracted top quark mass. Nonetheless, the observations presented here are expected to remain valid even after the inclusion of the aforementioned effects.

References

[1] I. I. Y. Bigi, M. A. Shifman, N. G. Uraltsev and A. I. Vainshtein, Phys. Rev. D **50** (1994), 2234-2246, doi:10.1103/PhysRevD.50.2234 arXiv:hep-ph/9402360 [hep-ph].

[2] M. Beneke and V. M. Braun, Nucl. Phys. B **426** (1994), 301-343, doi:10.1016/0550-3213(94)90314-X arXiv:hep-ph/9402364 [hep-ph].

[3] M. C. Smith and S. S. Willenbrock, Phys. Rev. Lett. **79** (1997), 3825-3828, doi:10.1103/PhysRevLett.79.3825 arXiv:hep-ph/9612329 [hep-ph].

[4] A. H. Hoang, C. Lepenik and M. Preisser, JHEP **09** (2017), 099, doi:10.1007/JHEP09(2017)099 arXiv:1706.08526 [hep-ph].

[5] A. H. Hoang, A. Jain, I. Scimemi and I. W. Stewart, Phys. Rev. Lett. **101** (2008), 151602, doi:10.1103/PhysRevLett.101.151602 arXiv:0803.4214 [hep-ph].

[6] T. Mäkelä, A. H. Hoang, K. Lipka and S. O. Moch, JHEP **23** (2020), 037 doi:10.1007/JHEP09(2023)037 arXiv:2301.03546 [hep-ph].

[7] A. H. Hoang, A. Jain, C. Lepenik, V. Mateu, M. Preisser, I. Scimemi and I. W. Stewart, JHEP **04** (2018), 003, doi:10.1007/JHEP04(2018)003 arXiv:1704.01580 [hep-ph].

[8] A. H. Hoang, C. Lepenik and V. Mateu, Comput. Phys. Commun. **270** (2022), 108145, doi:10.1016/j.cpc.2021.108145 arXiv:2102.01085 [hep-ph].

[9] U. Langenfeld, S. Moch and P. Uwer, Phys. Rev. D **80** (2009), 054009 doi:10.1103/PhysRevD.80.054009 arXiv:0906.5273 [hep-ph].

[10] M. Dowling and S. O. Moch, Eur. Phys. J. C **74** (2014) no.11, 3167, doi:10.1140/epjc/s10052-014-3167-x arXiv:1305.6422 [hep-ph].

[11] J. M. Campbell and R. K. Ellis, Nucl. Phys. B Proc. Suppl. **205-206** (2010), 10-15, doi:10.1016/j.nuclphysbps.2010.08.011 arXiv:1007.3492 [hep-ph].

[12] J. M. Campbell and R. K. Ellis, J. Phys. G **42** (2015) no.1, 015005, doi:10.1088/0954-3899/42/1/015005 arXiv:1204.1513 [hep-ph].

[13] S. Catani, S. Devoto, M. Grazzini, S. Kallweit and J. Mazzitelli, JHEP **08** (2020) no.08, 027 doi:10.1007/JHEP08(2020)027 arXiv:2005.00557 [hep-ph].

[14] CMS Collaboration, Phys. Lett. B **803** (2020), 135263, doi:10.1016/j.physletb.2020.135263 arXiv:1909.09193 [hep-ex].

[15] S. Alekhin, J. Blümlein, S. Moch and R. Placakyte, Phys. Rev. D **96** (2017) no.1, 014011, doi:10.1103/PhysRevD.96.014011 arXiv:1701.05838 [hep-ph].

[16] CMS Collaboration, Eur. Phys. J. C **80** (2020) no.7, 658, doi:10.1140/epjc/s10052-020-7917-7 arXiv:1904.05237 [hep-ex].

[17] Y. Kiyo, J. H. Kuhn, S. Moch, M. Steinhauser and P. Uwer, Eur. Phys. J. C **60** (2009), 375-386, doi:10.1140/epjc/s10052-009-0892-7 arXiv:0812.0919 [hep-ph].